Chapter IV
Results and Disscussions

4.1 Carriers Characterization

Fluidized-bed Fenton process lets ferric ion (Fe^{3+}), produced in the Fenton reaction, be transformed into iron oxide (FeOOH) onto carriers surface via the crystallization or sedimentation. This process combines the functions of homogeneous chemical oxidation (H_2O_2/Fe^{2+}), heterogeneous chemical oxidation (H_2O_2/FeOOH), fluidized-bed crystallization, and reductive dissolution of FeOOH. Heterogeneous Fenton process are of particular interest, since most of the iron remains in the solid phase. The solid phase is usually granular (metal oxides or sand), hence the treated water is easily separated from the iron. Mass titration method was selected to determinate the pzc of metal oxide. The addition subsequent portions of metal oxide to the water or an aqueous electrolyte solution might be acidified or may contain a base were carried out. The pH of the system changes gradually and approaches a constant value, which is the pzc in the case of pure oxide. This method is based on the postulate that pzc value is associated with pH of minimal solubility that allows to deduce pzc value from equilibrium pH of a concentration (Reymond, 1999).

In this study, aluminium oxide (Al_2O_3) and silica oxide (SiO_2) were use to compare the efficiency of nitrobenzene removal. Aluminium oxide had white color with ragged circle shape and average particle diameter is 2.5 mm. In previous study (Khunikakorn, 2006), the results from BET analysis revealed the surface area and average aperture information were 314 m^2/g and 10.89° respectively. From EDX analysis, this carrier consists of 49.97% of aluminum and 50.03% of oxygen by weight. Silica oxide was a light-brown grain shape and the particle diameter between 0.84 and 2.00 mm (Table 4.1).

Table 4.1 Comparison of different carriers (adsorption).

Carriers	Average Diameter (mm)	Surface area (m^2/g)	Pore size (m^2g)	pH_{pzc}
Al_2O_3	2.5	314	10.89	9.16
SiO_2	1.42	0.001462	0	6.35

From the experimental results, the pH_{pzc} of media, i.e., Al_2O_3 and SiO_2, are shown in the Figure 4.1a and 4.1b. The pH of suspensions was measured after 24 hrs of contact time. Experiments with de-ionized water (DI) represented the situation of no ionic strength whereas those with synthetic wastewater referred to the real situation. In case of Al_2O_3 (Figure 4.1(a)), the pH increased with increasing Al_2O_3 dosage. Regardless on the ionic strength, pH of both solutions increased rapidly at the first stage and was asymptote at 9.16. On the other hand, the pH of SiO_2 suspensions both with and without ionic strength dropped rapidly at the initial stage and leaned toward 6.35. This implies that the ionic strength causing by nitrobenzene and 0.025 M of Na_2SO_4 had no significant impact on pzc of the media. Reymond (1999) stated

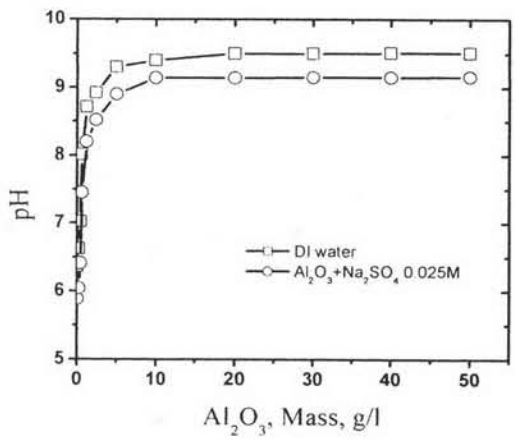

Figure 4.1a pH of experimental solution in Al_2O_3.

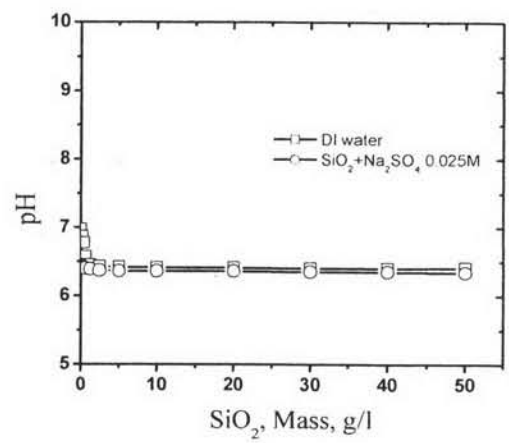

Figure 4.1b pH of experimental solution in SiO_2.

Figure 4.1 Measurement of point of zero charge of the carriers by mass titration.

that various ions could cause a screen effect on the surface charge but the pzc might not be altered if the ions were not specifically adsorbed on the carriers. These results indicated that the surfaces of both media were positively charged since the working pH range was 2.4-4.0 which was lower than the pzc.

The table 4.2 compares the pzc of metal oxide obtained in this study with those from other studies. It can be seen that the pzc of metal oxide obtained from this study was within the range reported by other researchers.

Table 4.2 Comparison point of zero charge of metal oxide.

Metal oxide	Description	Salt	pH_{pzc}	Source
Al_2O_3 SiO_2	0.01 of Nitrobenzene	0.025 M Na_2SO_4	9.16 6.35	This study
γ- Al_2O_3 SiO_2	American Cyanameid Cabot L90	- -	7.4 3.2	Noh and Schwarz (1988)
γ- Al_2O_3	-	KNO_3	7.5	Mustafa et al. (1998)
γ- Al_2O_3 SiO_2 (Aerosil) SiO_2 (Silica gel) SiO_2 (Tixosil) SiO_2 (Silica)	Degussa Procatayse Degussa Rhône-Poulene Rhône-Poulene Lobo	- - - - - -	6.9 8.4 3.5 6.2 6.7 10.6	Remond et al. (1999)
γ- Al_2O_3 (gibbsite)	-	-	8.1- 9.6	Jodin (2005)

4.2 Control Experiment (adsorption)

This experimental part aimed to determine the degradation of target compounds in fluidized-bed reactor deriving from each individual constituent via non-Fenton reaction. Figure 4.2 exhibits that nitrobenzene remaining obtained all control experiments versus time. The portion of nitrobenzene removed in 60 minutes by adsorption in the presence of H_2O_2 and Fe^{2+} were shown in Table 4.3.

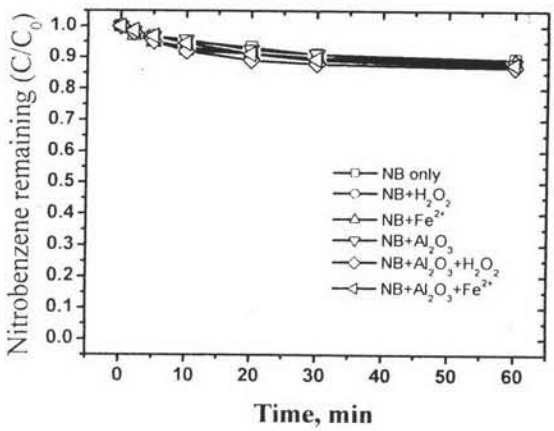

Figure 4.2a Nitrobenzene remaining with Al_2O_3.

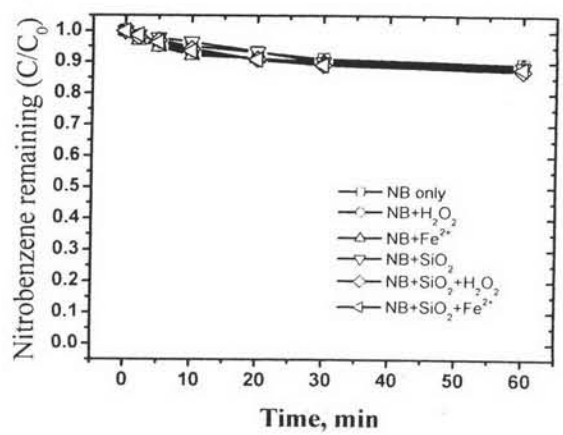

Figure 4.2b Nitrobenzene remaining with SiO_2.

Figure 4.2 Control experiment (adsorption) in fluidized-bed reactor. nitrobenzene = 0.01 M, Al_2O_3 = 100 g/l , SiO_2 = 100 g/l, Fe^{2+} = 0.001 M, H_2O_2 = 0.05 M and initial pH = 2.8.

Table 4.3 and Figure 4.2 exhibited that in control experiments, the removal efficiencies of nitrobenzene of carriers as Al_2O_3 system were nearly SiO_2 system in all control experiments, i.e., only 13.10% or less for nitrobenzene with aluminium oxide and 12.60% or less for nitrobenzene with silica oxide. The disappearance of nitrobenzene could be derived from many causes. Oxidation by H_2O_2 should be insignificant since nitrobenzene reaching a plateau while significant amount of H_2O_2 of greater than 87.5% still presented in the solution. It is believed that the adsorption onto the surface of carriers and apparatus was the major reason for the nitrobenzene

depletion. From these results, it implies that both of these target compounds could not be degraded effectively and rapidly without an involvement of hydroxyl radicals under the studied conditions.

Table 4.3 Nitrobenzene removal efficiency in control experiment (adsorption).

Carriers	% Nitrobenzene removal					
	only	+ H_2O_2	+ Fe^{2+}	+ Carriers	+ Carriers + H_2O_2	+ Carriers + Fe^{2+}
Al_2O_3	10.50	12.50	11.30	11.90	13.10	12.20
SiO_2	10.50	12.50	11.30	11.30	12.60	12.00

4.3 Comparison of different carriers

The comparison of different carriers between aluminuim oxide (Al_2O_3) and silica oxide (SiO_2) were investigated onto the oxidation of nitrobenzene in fluidized-bed Fenton process. As Fenton's reagent produce hydroxyl radical can lead to oxidize the organic compound, fluidized-bed Fenton can reduce the amount of iron oxide which is the drawback of Fenton process. The carriers which have different elements were operated in this scenario. The properties of the solid particles have major influence on fluidization (Rodriguez et al., 2000a). The dissimilar media properties could let the different removal efficiency behavior of target compounds. In previous study (Khunikakorn, 2006) aluminium oxide and silica oxide were used to be the carriers in fluidized-bed Fenton process effectively. In this study, the carriers which have different basic elements were operated in this scenario in order to determine the carrier was used for all experiment.

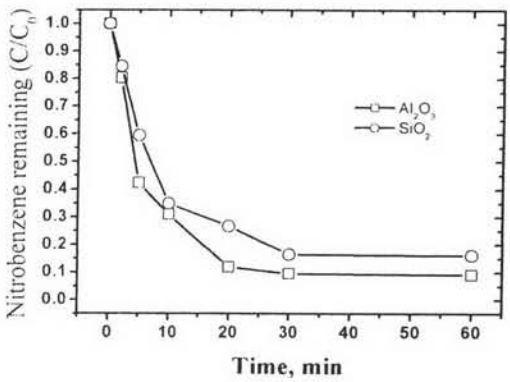

Figure 4.3a Nitrobenzene remaining with free chloride ions.

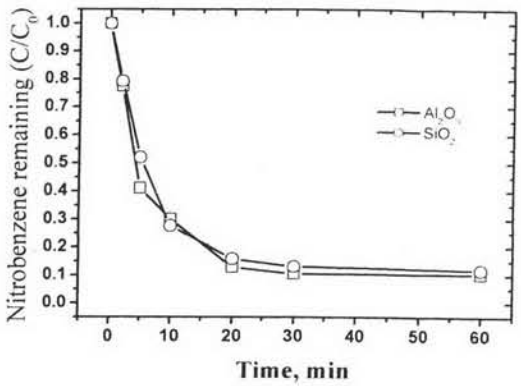

Figure 4.3b Nitrobenzene remaining with 0.0015 M of chloride ions.

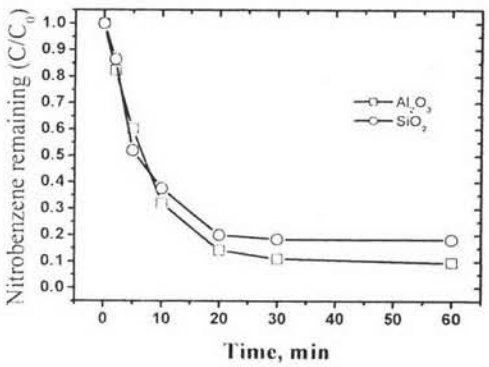

Figure 4.3c Nitrobenzene remaining with 0.02 M of chloride ions.

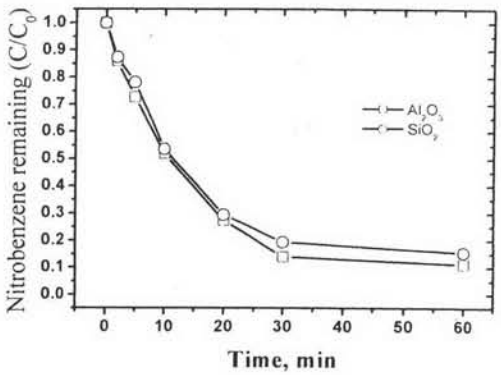

Figure 4.3d Nitrobenzene remaining with 0.2 M of chloride ions.

Figure 4.3 Comparison of different carriers; 0.01 M of nitrobenzene, 0.05 M of H_2O_2, 0.001 M of Fe^{2+}, 100 g/l of the carriers and initial pH 2.8.

Figure 4.3 compared the characteristics for nitrobenzene removal between Al_2O_3 and SiO_2. It was interesting in the scenario that the oxidation ofnitrobenzene were comparable for both carriers. Within the first 5 min, the characteristics of nitrobenzene was quite similar. The disappearance of nitrobenzene was rapidly at first 10 minutes. Nitrobenzene removal efficiency of the media as Al_2O_3 are higher than SiO_2 system when the chloride concentrations were increased.

The Al_2O_3 system, the removal efficiency of nitrobenzene in the presence of chloride ions at free, 0.0015M, 0.02M at 0.2M were 90.90%, 89.70%, 90.40% and 88.90% respectively. Together withthe SiO_2 system, the removal efficiency of nitrobenzene in the presence of chloride ions at free, 0.0015M, 0.02M at 0.2M were 83.90%, 88.20%, 81.70% and 84.50% respectively that were shown in Table 4.4.

Table 4.4 Nitrobenzene removal efficiency in comparison of different carriers.

Chloride ion (M)	Removal efficiency of nitrobenzene, %	
	Al_2O_3	SiO_2
0	90.90	83.90
0.0015	89.70	88.20
0.02	90.04	81.70
0.2	88.90	84.50

In conclusion, Al_2O_3 proved to be a better carrier for nitrobenzene oxidation in the fluidized-bed Fenton reactor system than the SiO_2. It is believed to be due to the higher pzc of Al_2O_3 which created more positive charged surface than SiO_2. This not only involved with the compound oxidation but also related to Fe^{2+} removal. Although the SiO_2 has higher specific surface area than Al_2O_3 due to smaller size, the removal of Fe^{2+} via iron crystallization onto carrier surface still occurred better with Al_2O_3. This research was investigated the oxidation rate nitrobenzene not adsorption, therefore, the chosen carrier was Al_2O_3. For the next scenario, the Al_2O_3 were conduced go through all expirement as the carrier in the system of fluidized-bed Fenton process.

4.4 pH optimization for Fluidized-bed Fenton process.

In this experiment, the optimization of pH for fluidized-bed Fenton process was examined for nitrobenzene oxidation in the fluidized-bed Fenton reactor. Typical

range for Fenton process is in the acidic range Consequently, it is essential to determine the optimum pH for the fluidized-bed Fenton process which can provide the best performance. In this scenario, the solution pH was operated initially at 2.0, 2.8, 3.5, 4.0, 5.0 and 6.0. In the Figure 4.4, the oxidation of nitrobenzene increased with decreasing of concentration of chloride ion. The removal efficiency of

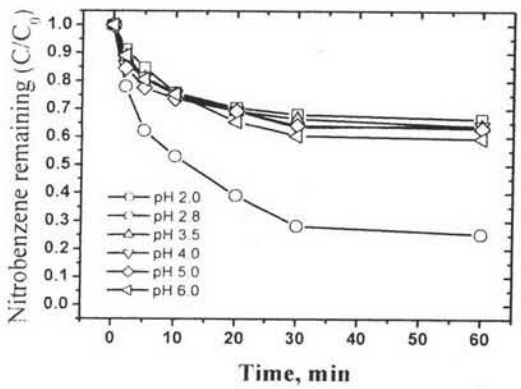

Figure 4.4a Nitrobenzene remaining with free chloride ions.

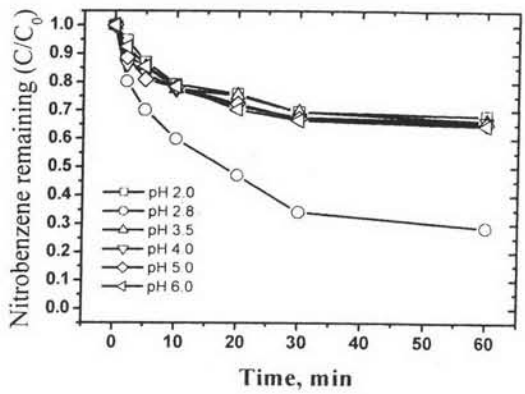

Figure 4.4b Nitrobenzene remaining with 0.02 M of chloride ions.

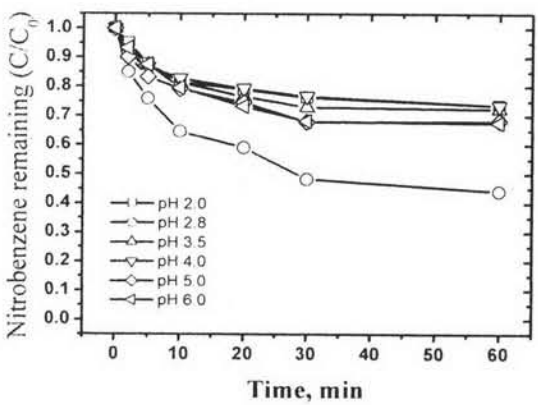

Figure 4.4c Nitrobenzene remaining with 0.20 M of chloride ions.

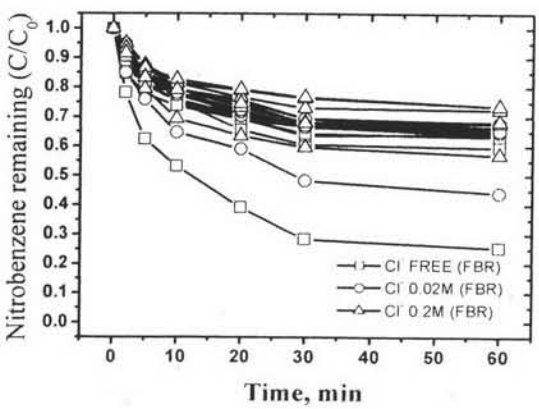

Figure 4.4d Nitrobenzene remaining with effect of chloride ions on pH.

Figure 4.4 Effect of pH; 0.01 M of nitrobenzene, 0.05 M of H_2O_2 0.25 mM of Fe^{2+}, 100 g/l of the aluminium oxide and initial pH 2.8.

nitrobenzene in the presence of free chloride ions concentration with pH was operated initially at 2.0, 2.8, 3.5, 4.0, 5.0 and 6.0 were 33.5%, 74.5%, 36.20%, 35.80%, 36.80% and 40.50% respectively. Together with the removal efficiency of nitrobenzene in the presence of 0.02 M of chloride ions concentration with pH was operated initially at 2.0, 2.8, 3.5, 4.0, 5.0 and 6.0 were 31.90%, 71.30%, 33.70%, 33.90%, 34.80% and 35.30% respectively and the removal efficiency of nitrobenzene in the presence of 0.2 M of chloride ions concentration with pH was operated initially at 2.0, 2.8, 3.5, 4.0, 5.0 and 6.0 were 26.40%, 55.90%, 27.60%, 26.40%, 31.70% and 32.30% respectively that were shown in Figure 4.4(a-c).

In this study, the effect of pH ranging from 2 to 6 was investigated to explore how chloride ions inhibited the Fenton reaction at different initial pH. The reactions at an initial pH of 2 and 6 are discussed first since there was an obvious inverse effect on the oxidation under those conditions. As shown in Figure 4.4d, only 74.50% of nitrobenzene was decomposed after 60 min of reaction in the Cl^--free reaction mixture. There was no significant difference in oxidation rate in the presence of 0.02 M of chloride ions. When the chloride concentration increased to 0.2 M, a slightly higher inhibition was observed. Based on the observation from these experiments, it can be found that oxidation of nitrobenzene cannot easily proceed at an initial pH. Experiments at an initial pH of 2.80 were carried out to compare with the other initial pH

Table 4.5 Pseudo-second order rate constants of nitrobenzene removal under different pH.

Cl - (M)	pH 2.0 $k \times 10^{-2}$ ($M^{-1}min^{-1}$)	pH 2.8 $k \times 10^{-2}$ ($M^{-1}min^{-1}$)	pH 3.5 $k \times 10^{-2}$ ($M^{-1}min^{-1}$)	pH 4.0 $k \times 10^{-2}$ ($M^{-1}min^{-1}$)	pH 5.0 $k \times 10^{-2}$ ($M^{-1}min^{-1}$)	pH 6.0 $k \times 10^{-2}$ ($M^{-1}min^{-1}$)
0	1.46800	7.90900	1.51800	1.67900	1.55000	2.05000
0.02	1.33400	3.24300	1.27400	1.40000	1.41800	1.63600
0.2	0.93600	2.19200	1.11100	1.16500	1.37500	1.49100

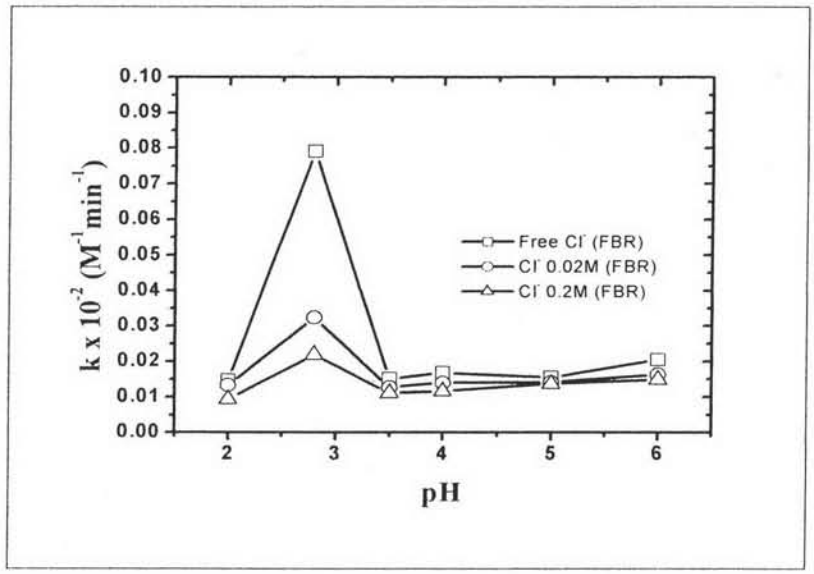

Figure 4.5 Effect of pH on pseudo-second order rate constants of nitrobenzene removal ; 0.01 M of nitrobenzene, 0.05 M of H_2O_2, 0.25 mM of Fe^{2+} and 100 g/l of the aluminium oxide.

The effect of chloride ions on the nitrobenzene oxidation should be reduced with increasing pH. For the purposes of comparing the oxidation rate, the concentration of nitrobenzene and reaction time was regressed by a second-order equation as shown in equation 4-1.

$$1/[A]=1/[A]_0+kt \qquad (4\text{-}1)$$

where $[A]$ is the nitrobenzene concentration at reaction time, t, $[A]_0$ is the initial concentration of nitrobenzene and k is the rate constant. The pseudo-second-order rate constants obtained under different experimental conditions are compared in Figure 4.5; the reaction time for these experiments was 30 minutes. The good fit of the linear model to the data (R>0.92 in all cases) provides strong evidence that the reaction is pseudo-second order with respect to nitrobenzene concentration. As expected, the nitrobenzene oxidation at high pH was not efficient; therefore, no significant difference was found when the reactions began at an initial pH of 5. Under the conditions of pH less than 5, the rate of aniline oxidation increased with increasing initial reaction pH regardless of chloride ions. As discussed above, the inhibition

effect by chloride ions should depend on the concentrations of Cl^- and H^+. Therefore, the difference in reaction rate should be significant at a lower pH as well as at a higher concentration of chloride ions. As shown in Table 4.5, the difference in rate constant between the curves for 0.02 M Cl^- and Cl^--free was obvious, and then it was reduced with an increasing of the initial pH. Additionally, the curve for 0.2 M Cl^- is almost parallel to that for 0.02 M, indicating that the inhibition effect depended on the chloride ion concentration as well as pH.

The inhibition effect of chloride ions increased with increasing chloride ion concentration ranging from 0 to 0.2 M. The oxidation efficiency of nitrobenzene by the Fenton process at an initial pH of 2.80 was highest. This research was investigated the oxidation rate nitrobenzene, the chosen pH was 2.80. For the next scenario, the initial pH of 2.80 was conduced go through all expirement in the system of fluidized-bed Fenton process.

4.5 Carriers size for Fluidized-bed Fenton process.

The purpose of the experimental study was to explore the comparison of different carrier sizes between 3.50 mm and 2.50 mm of aluminuim oxide (Al_2O_3) were investigated onto the oxidation of nitrobenzene in fluidized-bed Fenton process. As Fenton's reagent produce hydroxyl radical can lead to oxidize the organic compound, fluidized-bed Fenton can reduce the amount of iron oxide which is the drawback of Fenton process. The carriers which have different sizes were operated in this scenario. The properties of the solid particles have major influence on fluidization (Rodriguez et al., 2000a). The dissimilar media properties could let the different removal efficiency behavior of target compounds. In this study, the carrier was different sizes were operated in this scenario in order to determine the carrier size was used for all experiment.

Figure 4.6 compared the carrier sizes for nitrobenzene removal between 3.50 mm and 2.50 mm of aluminuim oxide (Al_2O_3). It was interesting in the scenario that the oxidation of nitrobenzene were comparable for both sizes. Within the first 5 min,

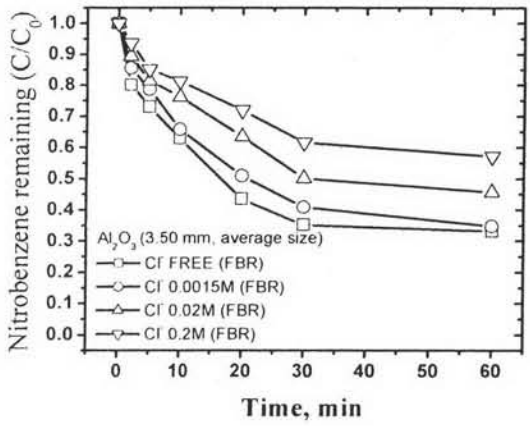

Figure 4.6a Nitrobenzene remaining with 3.50 mm of Al_2O_3.

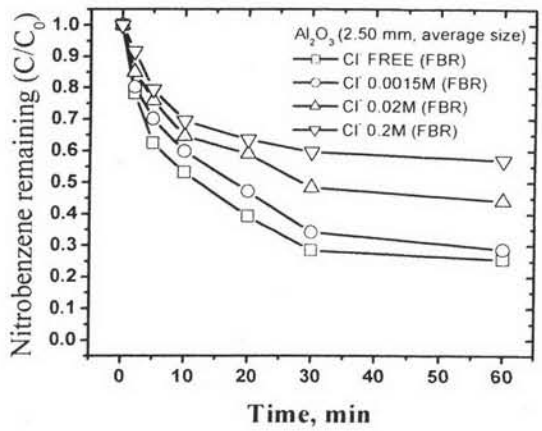

Figure 4.6b Nitrobenzene remaining with 2.50 mm of Al_2O_3.

Figure 4.6 Nitrobenzene oxidation in the presence of carriers size for fluidized-bed Fenton process; [Nitrobenzene]=1.0×10^{-3} M, [H_2O_2]=5×10^{-2} M, [Fe^{2+}]=2.5×10^{-4} M, initial pH 2.8.

the characteristics of nitrobenzene was quite similar. The disappearance of nitrobenzene was rapidly at first 10 minutes. Nitrobenzene removal efficiency of the carrier sizes as 2.50 mm are higher than 3.50 mm of Al_2O_3 and the nitrobenzene removal efficiency decreased with increasing the chloride concentrations. The removal efficiency of nitrobenzene of carrier size as 3.50 mm in the presence of chloride ions at free, 0.0015M, 0.02M at 0.2M were 66.80%, 65.20%, 54.30% and 42.80% respectively. Together with the carrier size as 2.50 mm, the removal efficiency of nitrobenzene in the presence of chloride ions at free, 0.0015M, 0.02M at 0.2M were 74.50%, 71.30%, 55.90% and 43.00% respectively that were shown in Table 4.6.

The pseudo-second-order rate constants obtained under different experimental conditions are compared in Table 4.6.; the reaction time for these experiments was 30 minutes. The good fit of the linear model to the data (R>0.95 in all cases) provides strong evidence that the reaction is pseudo-second order with respect to nitrobenzene concentration.

Table 4.6 Pseudo-second order rate constants of nitrobenzene removal under different carrier sizes.

Cl- (M)	Al_2O_3 3.50 mm		
	% Nitrobenzene removal	k ($x10^{-2}M^{-1}min^{-1}$)	R
0	66.80	6.00700	0.99696
0.0015	65.20	4.68700	0.99898
0.02	54.30	3.08200	0.99161
0.2	42.80	1.94300	0.99235
Cl- (M)	Al_2O_3 2.50 mm		
	% Nitrobenzene removal	k ($x10^{-2}M^{-1}min^{-1}$)	R
0	74.50	7.90900	0.99517
0.0015	71.30	5.94500	0.99276
0.02	55.90	3.24300	0.97891
0.2	43.00	2.18700	0.94681

In conclusion, carrier sizes as 2.50 mm proved to be a better carrier for nitrobenzene oxidation in the fluidized-bed Fenton reactor system than the carrier sizes as 3.50 mm. Carrier sizes as 2.50 mm is believed to be due to the higher carrier surface. The removal of Fe^{2+} via iron crystallization onto carrier surface still occurred better with carrier sizes as 3.50 mm. This research was investigated the oxidation rate nitrobenzene, the chosen carrier size was 2.50 mm of Al_2O_3. For the next scenario, the 2.50 mm of Al_2O_3 were conduced go through all expirement as the carrier in the system of fluidized-bed Fenton process.

4.6 Comparison between Traditional Fenton and Fluidized-bed Fenton Processes

To compare the performance of traditional and fluidized-bed Fenton processes, the optimum conditions from previous sections have been employed, i.e., using Al_2O_3 as the carrier and working at the optimum pH of each scenario. According to comparison between FBR and traditional Fenton process on the oxidation of nitrobenzene in fluidized-bed reactor with condition; 0.01 M of

nitrobenzene, 0.05 M of H_2O_2 and 0.001 M of Fe^{2+}, the result show that the removal efficiency of nitrobenzene as shown in Figure 4.7.

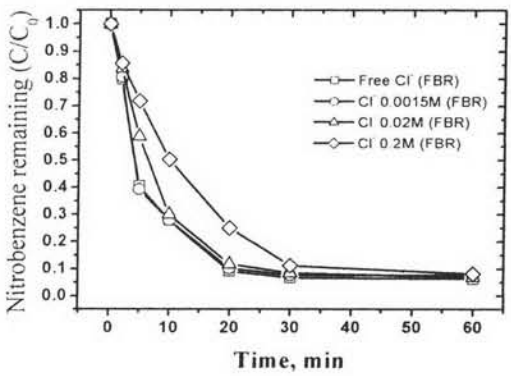

Figure 4.7a Nitrobenzene remaining with Fluidized-bed Fenton Process.

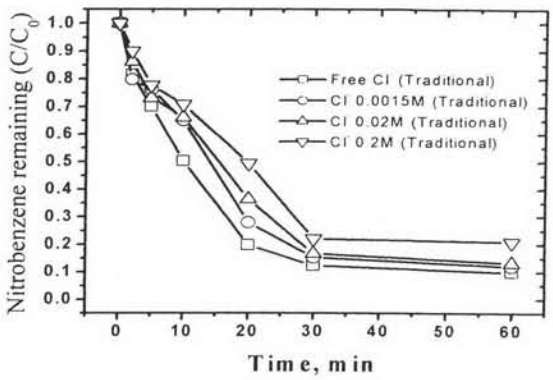

Figure 4.7b Nitrobenzene remaining with Traditional Fenton Process.

Figure 4.7 Comparison between Traditional Fenton and Fluidized-bed Fenton Process; 0.01 M of NB, 0.05 M of H_2O_2, 0.001 M of Fe^{2+}, 100 g/l of the media and initial pH 2.8.

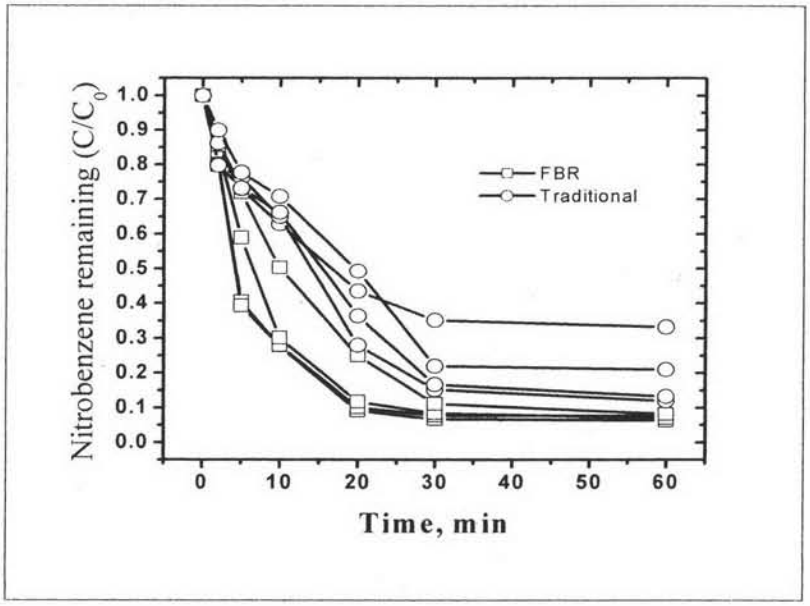

Figure 4.8 Comparison of nitrobenzene oxidation with between FBR and traditional Fenton process.

Figure 4.7-4.8 compared the nitrobenzene oxidation between fluidized-bed Fenton process and traditional Fenton process. It was interesting in the scenario that the oxidation of nitrobenzene were comparable. Within the first 2 minutes, the characteristics of nitrobenzene was quite similar. The disappearance of nitrobenzene was rapidly at first 5 minutes. Nitrobenzene removal efficiency of the fluidized-bed Fenton process are higher than the traditional Fenton process and the nitrobenzene removal efficiency decreased with increasing the chloride concentrations. The removal efficiency of nitrobenzene in fluidized-bed Fenton process, in the presence of chloride ions at free, 0.0015M, 0.02M at 0.2M were 93.70%, 92.40%, 93.00% and 91.80% respectively. Together with the traditional Fenton process, the removal efficiency of nitrobenzene in the presence of chloride ions at free, 0.0015M, 0.02M at 0.2M were 66.80%, 88.00%, 86.70% and 79.00% respectively that were shown in Table 4.7.

The pseudo-second-order rate constants obtained under different experimental conditions are compared in Table 4.7; the reaction time for these experiments was 30 minutes. The good fit of the linear model to the data (R>0.92 in all cases) provides strong evidence that the reaction is pseudo-second order with respect to nitrobenzene concentration.

Table 4.7 Pseudo-second order rate constants of nitrobenzene removal under different process between Traditional Fenton and Fluidized-bed Fenton Processes.

Cl^- (M)	FBR			Traditional		
	%Nitrobenzene removal	k (x 10^{-2} $M^{-1}min^{-1}$)	R	%Nitrobenzene removal	k (x 10^{-2} $M^{-1}min^{1}$)	R
0	93.70	49.21100	0.98888	66.80	6.00700	0.99696
0.0015	92.40	41.95900	0.99002	88.00	17.93400	0.96388
0.02	93.00	38.18500	0.99159	86.70	15.43200	0.94156
0.2	91.80	25.07500	0.95354	79.00	10.66200	0.92419

In conclusion, fluidized-bed Fenton process proved to be a better process for nitrobenzene oxidation in the fluidized-bed reactor than traditional Fenton process. The removal of Fe^{2+} via iron crystallization onto carrier surface still occurred in

fluidized-bed Fenton process. This research was investigated the oxidation rate nitrobenzene, the chosen process was fluidized-bed Fenton. For the next scenario, the fluidized-bed Fenton process were conduced go through all expirement.

4.7 Effect of chloride ions on the oxidation of nitrobenzene by fluidized-bed Fenton process in the presence of ferrous concentration.

The effectc of ferrous ion concentration on the oxidation of nitrobenzene by fluidized-bed Fenton process are illustrated in Figure 4.9. Fe^{2+} played an important role in catalyzing H_2O_2 to produce the $OH^{\bullet}$ via Fenton reaction. Based on the discussion in chapter 2, a complex reaction might be the primary cause of inhibition of the Fenton reaction. Therefore, experiments with increased initial ferrous ion concentration were carried out to investigate the inhibition mechanism. The oxidation rate of nitrobenzene with different initial ferrous ion concentrations ranging from 2.5×10^{-4} M to 1.0×10^{-3} M. The amount of nitrobenzene in the reaction mixtures decreased with increasing initial ferrous concentration.

Figure 4.9a, the removal efficiency of nitrobenzene in fluidized-bed Fenton process, as 0.001 M of ferrous ion concentration in the presence of chloride ions at free, 0.0015M, 0.02M at 0.2M were 90.90%, 89.70%, 90.04% and 88.90% respectively.

Figure 4.9b, the removal efficiency of nitrobenzene in fluidized-bed Fenton process, as 0.0005 M of ferrous ion concentration in the presence of chloride ions at free, 0.0015M, 0.02M at 0.2M were 93.90%, 93.10%, 89.20% and 79.60% respectively.

Figure 4.9c, the removal efficiency of nitrobenzene in fluidized-bed Fenton process, as 0.001 M of ferrous ion concentration in the presence of chloride ions at free, 0.0015M, 0.02M at 0.2M were 92.00%, 91.90%, 87.50% and 74.60% respectively.

Figure 4.9d, the removal efficiency of nitrobenzene in fluidized-bed Fenton process, as 0.001 M of ferrous ion concentration in the presence of chloride ions at free, 0.0015M, 0.02M at 0.2M were 74.50%, 71.30%, 55.90% and 43.40%

respectively that were shown in Figure 4.9.

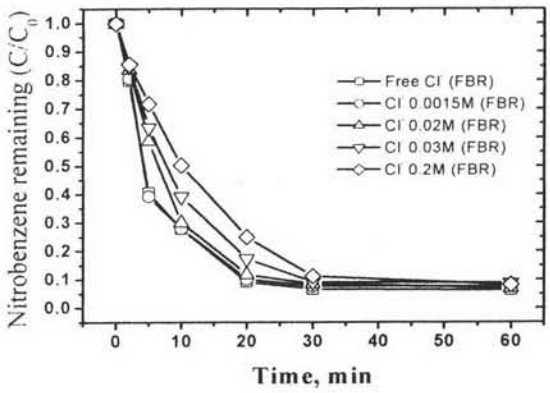

Figure 4.9a Nitrobenzene remaining with 0.001 M of Fe^{2+}.

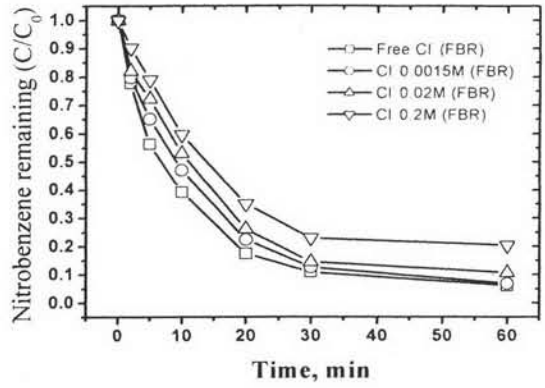

Figure 4.9b Nitrobenzene remaining with 0.0005 M of Fe^{2+}.

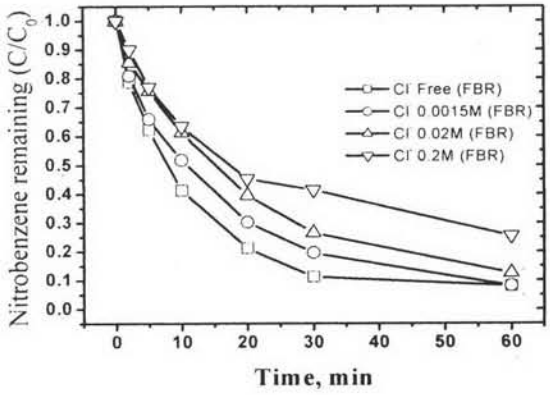

Figure 4.9c Nitrobenzene remaining with 0.000375 M of Fe^{2+}.

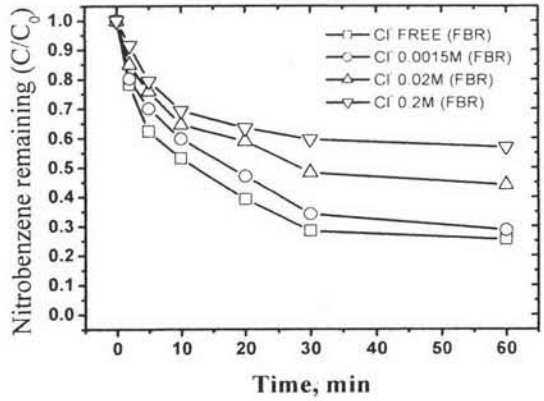

Figure 4.9d Nitrobenzene remaining with 0.00025 M of Fe^{2+}.

Figure 4.9 Effect of Fe^{2+} on oxidation of nitrobenzene in fluidized-bed Fenton process ; Fe^{2+} dosage: 0.001, 0.0005, 0.000375 and 0.00025 M with parameter conditions; 0.01 M of nitrobenzene, 0.001 M of H_2O_2, 100 g/l of the Al_2O_3 and initial pH 2.8.

The pseudo-second-order rate constants obtained under different experimental conditions are compared in Table 4.8.; the reaction time for these experiments was 30 minutes. The good fit of the linear model to the data (R>0.97 in all cases) provides

strong evidence that the reaction is pseudo-second order with respect to nitrobenzene concentration.

Table 4.8 Pseudo-second order rate constants of nitrobenzene removal under different pH.

Cl^- (M)	0.001 M of Fe^{2+}	0.0005 M of Fe^{2+}	0.000375 M of Fe^{2+}	0.00025 M of Fe^{2+}
	k x 10^{-2} ($M^{-1}min^{-1}$)	k x 10^{-2} ($M^{-1}min^{-1}$)	k x 10^{-2} ($M^{-1}min^{-1}$)	k x 10^{-2} ($M^{-1}min^{-1}$)
0	33.99400	27.41600	25.86800	7.90900
0.0015	30.41200	22.69000	13.47400	5.94500
0.02	28.71600	19.19000	9.03200	3.24300
0.2	25.45600	11.22000	4.96200	2.19200

The Fenton reaction is extremely sensitive to chloride ions remaining in the solution. This inhibition may be due to complexation and radical scavenging. As shown in equation 4-1 and 4-2, chloride ions create competition between hydroxyl radicals and organics, leading to the inhibition of oxidation. This may result in a complex reaction with ferric ions. In addition, chloride ions also interact with hydroxyl radicals, so that chloride ions compete with organic compounds for hydroxyl radicals, and therefore slow down the oxidation rate (Liao et al., 2001).

$$\cdot OH + Cl^- \leftrightarrow HOCl^-\cdot \qquad (4\text{-}2)$$

$$HOCl^-\cdot + H^+ \rightarrow Cl\cdot + H_2O \qquad (4\text{-}3)$$

According to the effect of complexation, Cl^- may undergo a complex reaction with ferrous and ferric ions, which impedes the reaction causing hydroxyl radicals to be produced. The complex reactions are shown in equation 4-3, 4-4, 4-5, 4-6 and 4-7 (Benjamin, 2002).

$$Fe^{2+} + Cl^- \rightarrow FeCl^+ \log K_1 = 0.90 \qquad 4\text{-}3$$

$$FeCl^+ + Cl^- \rightarrow FeCl^0{}_2 \log K_2 = 0.04 \qquad 4\text{-}4$$

$$Fe^{3+} + Cl^- \rightarrow FeCl_2 \log K_1 = 3.92 \qquad 4\text{-}5$$

$$FeCl^{2+} + Cl^- \rightarrow FeCl^+{}_2 \log K_2 = 5.42 \qquad 4\text{-}6$$

$$FeCl^+{}_2 + Cl^- \rightarrow FeCl^0{}_3 \log K_3 = 1.13 \qquad 4\text{-}7$$

Based on the reactions above, the Fenton reaction has been inhibited because the ferrous and ferric complexes cannot catalyze hydrogen peroxide to produce hydroxyl radicals as efficiently as their free types. At the initial stage of the Fenton reaction, the iron species is ferrous ion. The values of $\log K_1$ and $\log K_2$ for the ferrous ions complex together with the chloride ions are much lower than those for the ferric type. This indicates that free ferrous ions still exist in the solution and the production of hydroxyl radicals can indeed be carried out. When the Fenton reaction was at the

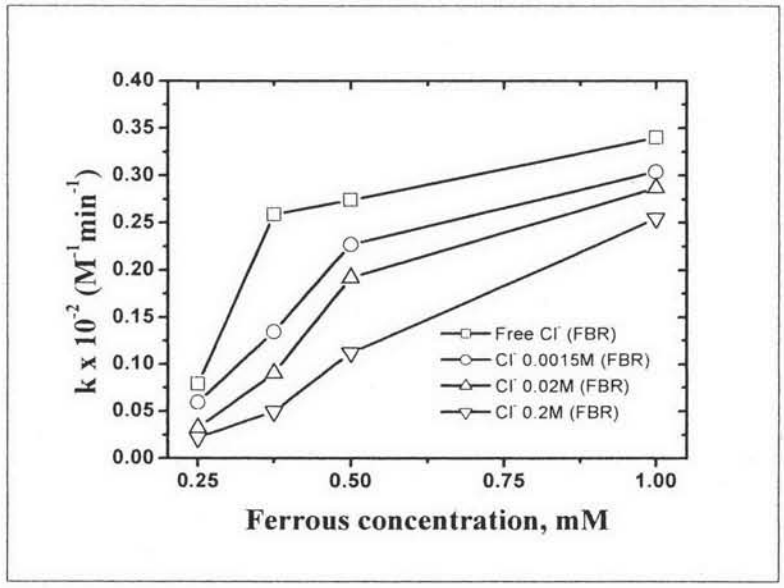

Figure 4.10 Effect of ferrous ions on pseudo-second order rate constants of nitrobenzene removal.

Fe^{3+}/H_2O_2 stage, according to equation 4-3, 4-4, 4-5, 4-6 and 4-7, it was found that most ferric ions formed the Fe–Cl complex. Therefore, at this stage, the oxidation rate of nitrobenzene decreased as the chloride ions concentration increased. However, there was almost no difference in the amount of nitrobenzene remaining after 60 minutes of reaction when the chloride ions concentrations were in the range of 0–1.5×10^{-3} M. This reveals that the inhibition can be overcome by extending the reaction time if the concentration of chloride ions is less than 0.2 M. Therefore, the subsequent experiments were carried out at high chloride concentrations.

4.8 Kinetic Determination for Fluidized-bed Fenton Process

It is important to mention that the kinetic determination in this section was performed based on the optimum pH, nitrobenzene and aluminium oxide at 2.8, 0.01 M and 100 g/l respectively, which obtained from previous sections.

4.8.1 Effect of ferrous

In this study, the initial oxidation rate of nitrobenzene was enchanced significantly as the Fe^{2+} increased from 0.25 to 1.0 mM as shown in Figure 4.11.

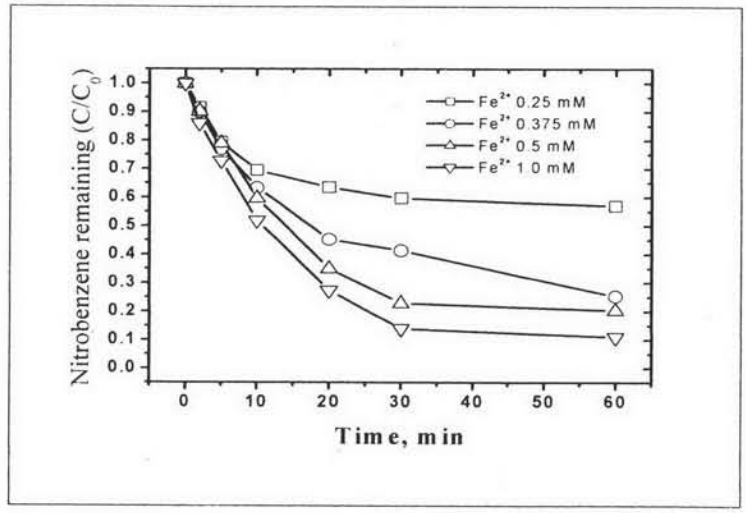

Figure 4.11 Effect of ferrous; 0.01 M of NB, 0.05 M of H_2O_2, 0.2 M of Cl^- and initial pH 2.8.

The overall removal efficiencies were between 43 to 90 % for fluidized-bed Fenton process. The oxidation rate of nitrobenzene with different initial ferrous ion concentrations ranged from 0.25 to 1.0 mM. The remaining amount of nitrobenzene in the reaction mixtures decreased with increasing initial ferrous concentration.

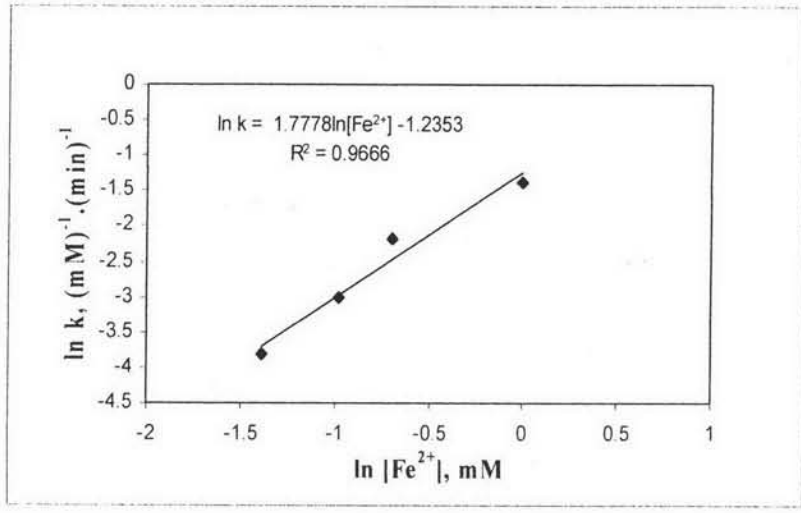

Figure 4.12 Relationship between nitrobenzene removal rate and Fe^{2+} concentration; 0.01 M of NB, 0.05 M of H_2O_2, 0.2 M of Cl^- and initial pH 2.8.

Furthermore, analysis on the initial rates showed a linear-dependent relationship with initial ferrous concentration as shown in Figure 4.12. Therefore, the kinetics can be described by the following equation :

$$d[NB]/dt = - k_{Fe^{2+}} [Fe^{2+}]^{1.78} \quad \text{.....(4-8)}$$

where "$k_{Fe^{2+}}$" is the rate constant

4.8.2 Effect of hydrogen peroxide

Fenton's chemistry involved a complex collection of reaction pathways. Its utility as an oxidizing system relied on the formation of hydroxyl radical ($OH^{\bullet}$) from

H_2O_2, through the reduction and oxidation (redox) cycles of iron (Fe) and a series of radicals propagation and termination reactions. In this part, various H_2O_2 concentrations of 0.025, 0.050, 0.075 and 0.100 M were employed to observe the effect on degradation rate of target compounds.

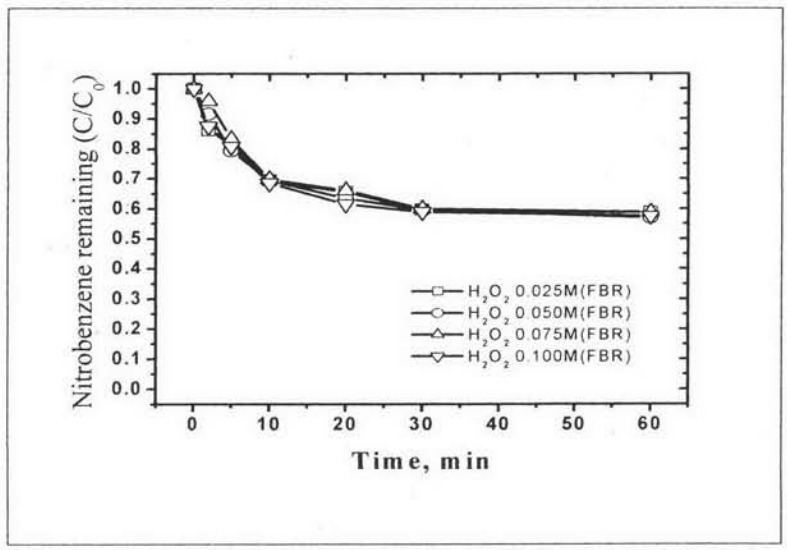

Figure 4.13 Effect of hydrogen peroxide; 0.01 M of NB, 0.25 mM of Fe^{2+},0.2 M of Cl^-, 100 g/l of the media and initial pH 2.8.

The removal efficiency of nitrobenzene in fluidized-bed Fenton process in the effects of H_2O_2 at 0.025M, 0.050M, 0.075M at 0.100M were 42.50%, 43.00%, 41.30% and 41.20%. The effects of H_2O_2 dosage on the degradation of nitrobenzene were shown in Figure 4.12. The results show that the amount of hydrogen peroxide added in the reaction mixture was also considered in the presence of a high concentration of chloride ions. As shown in Figure 4.13, when the concentration of ferrous ion was from 2.5×10^{-4}M to 1.0×10^{-1}M of hydrogen peroxide were added in the reaction mixtures in order to explore its effect on the reaction. Results show that increasing hydrogen peroxide concentration was not significant.

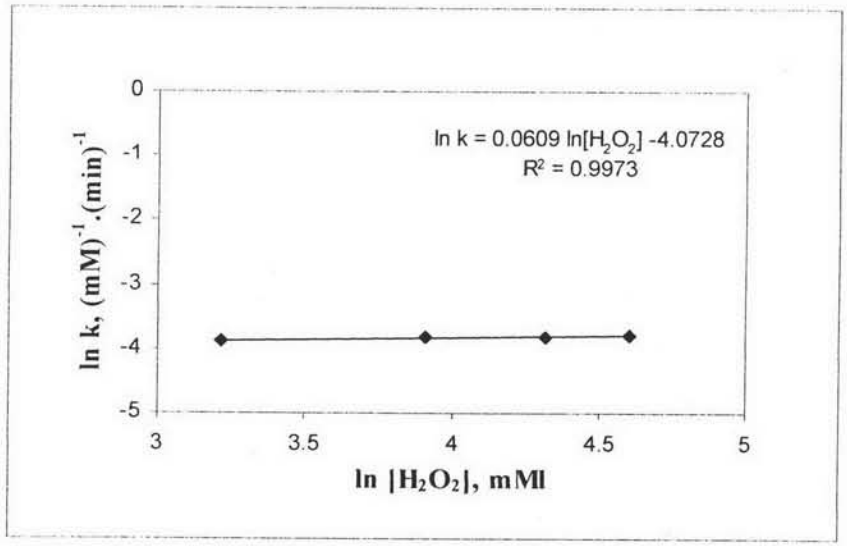

Figure 4.14 Relationship between nitrobenzene removal rate and H_2O_2 concentration; 0.01 M of NB, 0.25 mM of Fe^{2+},0.2 M of Cl^-, 100 g/l of the media and initial pH 2.8.

Furthermore, analysis on the initial rates showed a linear-dependent relationship with initial hydrogen peroxide concentration as shown in Figure 4.14. Therefore, the kinetics can be described by the following equation :

$$d[NB]/dt = - k_{H^2O^2} [H_2O_2]^{0.06} \quad \text{.....(4-9)}$$

where "$k_{Fe^{2+}}$" is the rate constant

4.8.3 Effect of chloride ions

In this study, the initial oxidation rate of nitrobenzene was enchanced significantly as the chloride ions increased from 0.00 to 0.20 M as shown in Figure 4.15. The removal efficiency of nitrobenzene in fluidized-bed Fenton process, as 0.001 M of ferrous ion concentration in the presence of chloride ions at free, 0.0015M, 0.02M at 0.2M were 74.50%, 71.30%, 55.90% and 43.40%.

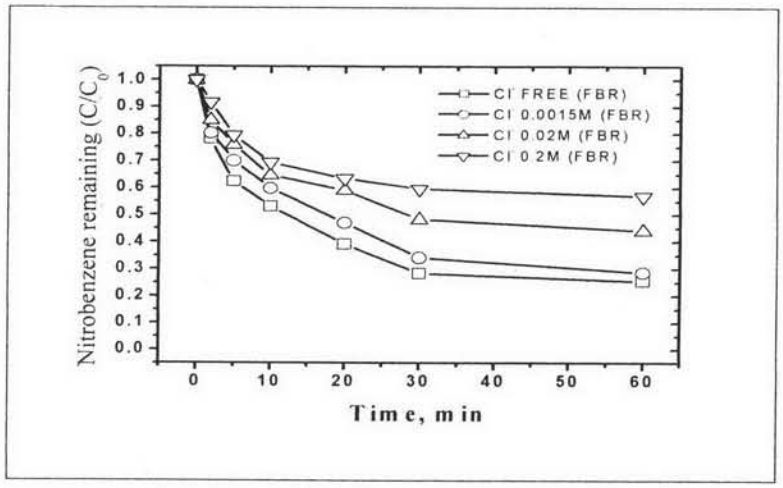

Figure 4.15 Effect of chloride ions; 0.01 M of NB, 0.25 mM of Fe^{2+},0.05 M of H_2O_2, 100 g/l of the media and initial pH 2.8.

Furthermore, analysis on the initial rates showed a linear-dependent relationship with initial chloride ions concentration as shown in Figure 4.16. Therefore, the kinetics can be described by the following equation :

$$d[NB]/dt = - k_{Cl^-} [Cl^-]^{-0.2315} \quad \text{.....(4-10)}$$

where "$k_{Fe^{2+}}$" is the rate constant

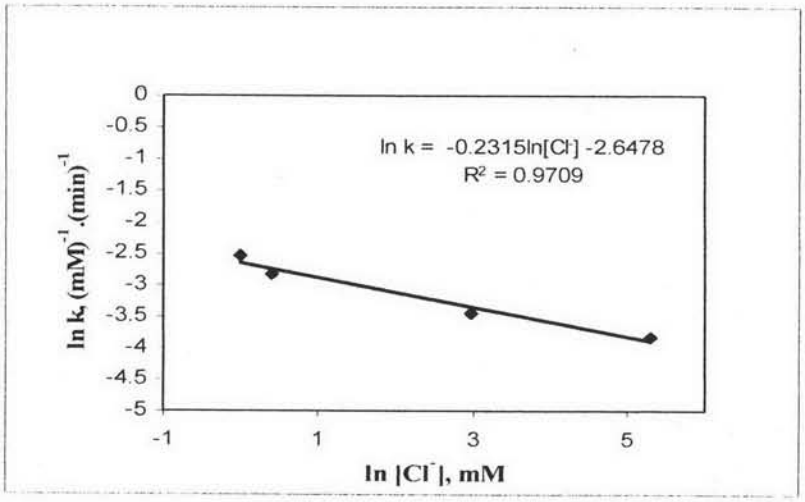

Figure 4.16 Relationship between nitrobenzene removal rate and chloride ions concentration; 0.01 M of NB, 0.25 mM of Fe^{2+},0.05 M of H_2O_2, 100 g/l of the media and initial pH 2.8.

4.8.4 Overall decomposition kinetics

After all the individual reaction orders with respect to each reactants where known, the overall rate nitrobenzene oxidation by fluidized-bed Fenton process can be written as :

$$d[NB]/dt = - k [Fe^{2+}]^{1.78} [H_2O_2]^{0.06} [Cl^-]^{-0.23} [NB]^2 \quad \text{.....(4-11)}$$

where "k" is the overall rate constsnt for nitrobenzene oxidation within the concentration of Fe^{2+} of 0.25 to 0.1 mM, H_2O_2 0.025 to 0.100 mM and chloride ions increased from 0.00 to 0.20 M.

These "k" values can be determined by the use of a non-linear least square regression which minimizing the sum of error squares between the measured rates obtained from the experiments and the calculated rate generated by the above equations. By giving all these parameters conditions from the experiments, the final rate equations became:

$$d[NB]/dt = - 0.7039 [Fe^{2+}]^{1.78} [H_2O_2]^{0.06} [Cl^-]^{-0.23} [NB]^2 \quad \text{.....(4-12)}$$

This rate equation is valid under the experiment conditions as follow: pH 2.8, aluminium oxide 100 g/l, initial Fe^{2+} concentration between 0.25 to 0.1 mM, initial H_2O_2 concentration between 0.025 to 0.100 mM , initial nitrobenzene concentration 0.01 M and chloride ions concentration between 0.00 to 0.20 M at room temperature.

4.9 Effect of carriers on the oxidation of nitrobenzene in fluidized-bed reactor.

4.9.1 Effect of initial amount of aluminium oxide media on the oxidation of nitrobenzene in FBR.

The purpose of the experimental study was to explore the effect of initial amount of aluminium oxide was investigated onto the oxidation of nitrobenzene in

fluidized-bed Fenton process. As Fenton's reagent produce hydroxyl radical can lead to oxidize the organic compound, fluidized-bed Fenton can reduce the amount of iron oxide which is the drawback of Fenton process. The aluminium oxide which have different quantity were operated in this scenario. It was interesting in the scenario that the oxidation of nitrobenzene, within the first 5 min, the characteristics of nitrobenzene was quite similar. The disappearance of nitrobenzene was rapidly at first 10 minutes. The removal efficiency of nitrobenzene of initial amount of aluminium

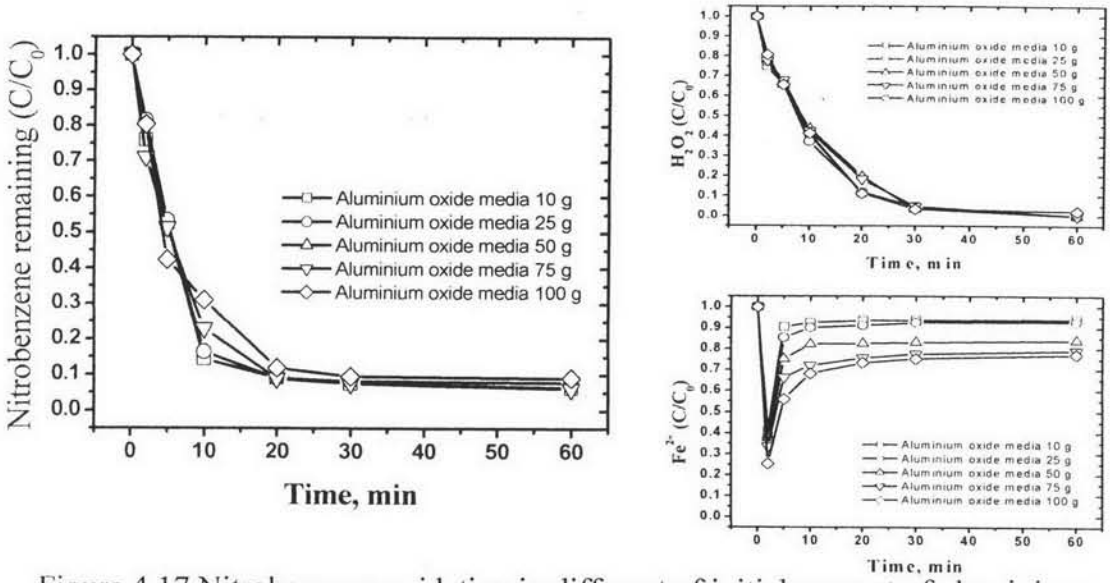

Figure 4.17 Nitrobenzene oxidation in different of initial amount of aluminium oxide media: 0.01 M of NB, 0.05 M of H_2O_2, 0.001 M of Fe^{2+} and initial pH 2.8.

oxide at 10, 25, 50, 75 and 100 grams were 93.60%, 92.20%, 94.20%, 93.90 and 90.90% respectively that were shown in Figure 4.17, presents the effect of initial amount of aluminium oxide media on the oxidation of nitrobenzene. It is interesting to find that instead of promoting effect, the increase of initial amount of aluminium oxide media does not improve the oxidation of nitrobenzene. In addition the residual of H_2O_2 was not significant different with higher media dosages as shown in H_2O_2 remaining. In contrast, the profile of Fe^{2+} was quite different. the residual of Fe^{2+} was decreased with increasing of media dosage as shown in ferrous remaining. It might be due to the precipitation of iron on the surface of media. Generally speaking, the higher

dosage of media will have higher surface area available. As a result, it can be said that the increasing of media dosages was not effect to the oxidation of nitrobenzene.

4.9.2 Effect of reusability of aluminium oxide media on the oxidation of nitrobenzene in FBR.

To investigate the effect of reusability of aluminium oxide media on the oxidation of nitrobenzene in FBR. The oxidation of nitrobenzene, within the first 5 min, the characteristics of nitrobenzene was quite similar. The disappearance of nitrobenzene was rapidly at first 10 minutes. The removal efficiency of nitrobenzene of reusability of aluminium oxide at first, sencond, third, fourth and fifth cycles were 94.00%, 94.30%, 94.20%, 93.60 and 91.30% respectively that were shown in Figure 4.18. In addition the residual of H_2O_2 was not significant different with higher media dosages as shown in H_2O_2 remaining. In contrast, the profile of Fe^{2+} was quite different. the residual of Fe^{2+} was decreased with increasing of media dosage as shown in ferrous remaining.

Fenton reaction (H_2O_2/ Fe^{2+}) can promote the non-selective oxidant as $OH^{\cdot}$ leading to the degradation of aromatic organic containing in the wastewater. In the process, Fe^{3+} is generated and can crystallize onto carrier surface. It is of interest to investigate on the reuse ability of Al_2O_3 which can lead to the reduction in sludge volume. Al_2O_3 were reused up to 5 cycles under the same conditions. Figure 4.18 summarizes all aspect of the FBR with reused Al_2O_3. It was found that the FBR behavior regarding on nitrobenzene were quite similar for all five cycles. Lo et al., (1997) mentioned that the optimum pH and pore of specific area on the surface media played the important factor of attachment iron oxide coating.

However, the impact of specific area on the surface of Al_2O_3 was not obvious in this study. This might be due to the differences in system configuration and

conditions. It can be seen that portion of iron gradually increased with reused cycle. However, the appearance of Al_2O_3 were very small changed in case of size and figure due to crystallization of iron induce the carriers hardness and the absent of iron was slightly when compare with weight. These findings imply that the iron oxide coated Al_2O_3 can be reused successfully in the fluidized-bed Fenton process.

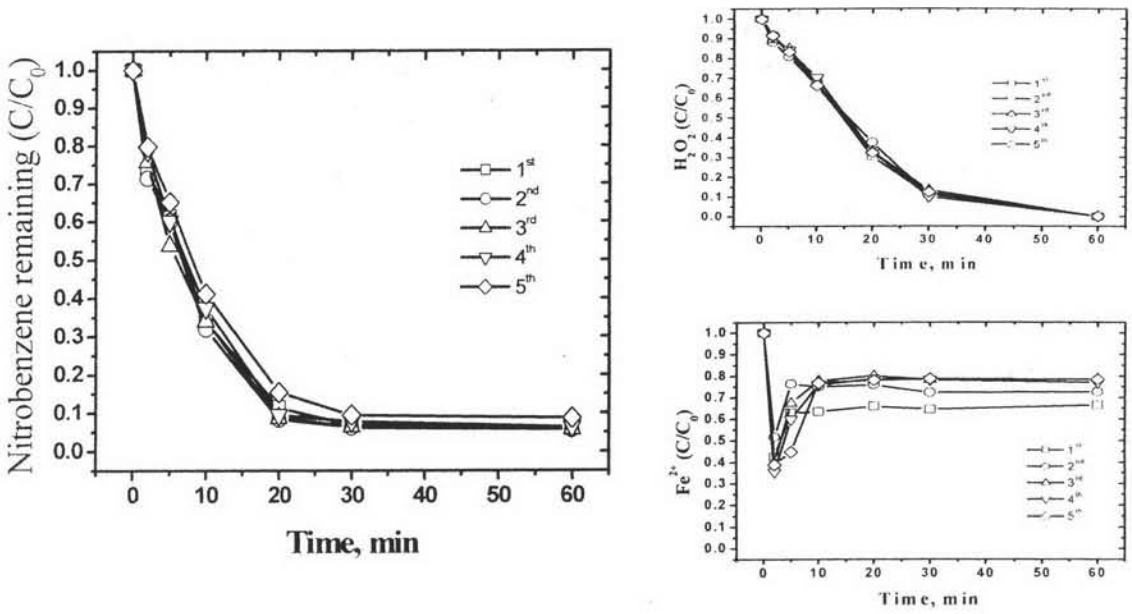

Figure 4.18 Reusability of aluminium oxide media on the oxidation of nitrobenzene in FBR. ; 0.01 M of NB, 0.05 M of H_2O_2, 0.001 M of Fe^{2+}, 100 g/l of the media and initial pH 2.8.

4.9.3 Iron crystallization

In this part, carriers was used in the fluidized-bed reactor in order to investigate the effect of ferrous ions on the oxidation of nitrobenzene. Ferrous concentration was at 0.00025 M - 0.001 M. Therefore, after 60 minutes, the iron remaining in the solution was slightly decreased. The higher ferrous concentration was use to determine the impact of crystallization iron that coating onto surface of aluminium oxide (Al_2O_3) in fluidized-bed Fenton process with the condition: nitrobenzene = 0.01 M, H_2O_2 = 0.05 M, carriers (Al_2O_3) = 100 g/l and initial pH 2.8. It

was found that there was difference regarding on the crystallization among ferrous concentration 0.00025 M to 0.001 M.

At the condition with high ferrous concentration, the total iron remaining was lower than that at the condition with low ferrous concentration. The total iron remaining was lower that means iron in the solution transformed into iron oxide (FeOOH) on to carrier surface via crystallization. Therefore, this process combines the functions of homogeneous chemical oxidation (H_2O_2, Fe^{2+}), heterogeneous chemical oxidation (H_2O_2, FeOOH), fluidized-bed crystallization, and reductive dissolution of FeOOH.

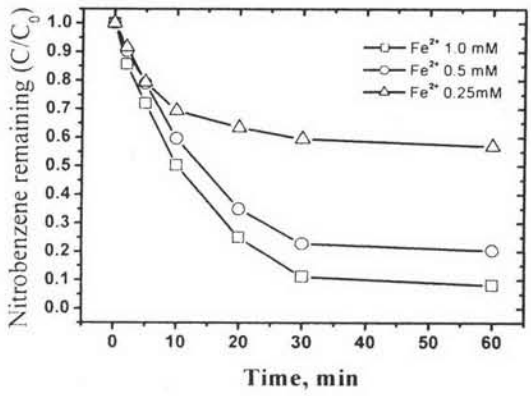

Figure 4.19a Nitrobenzene remaining.

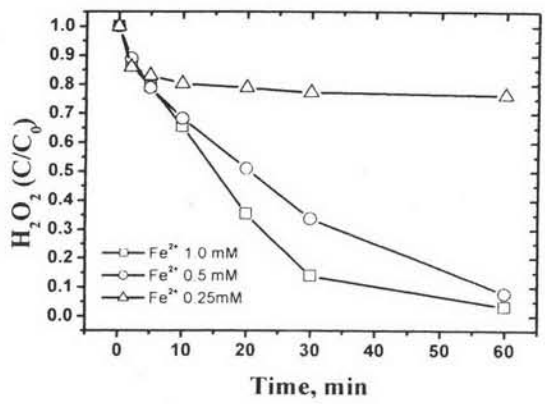

Figure 4.19b H_2O_2 remaining.

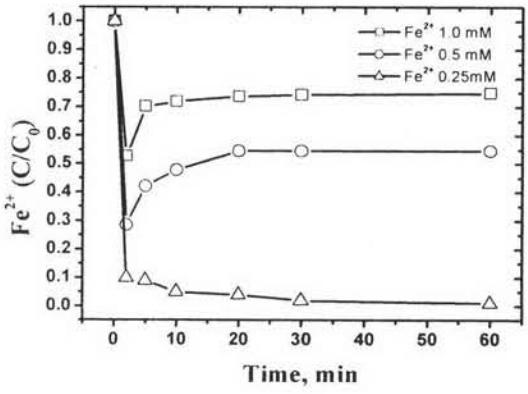

Figure 4.19c Fe^{2+} remaining.

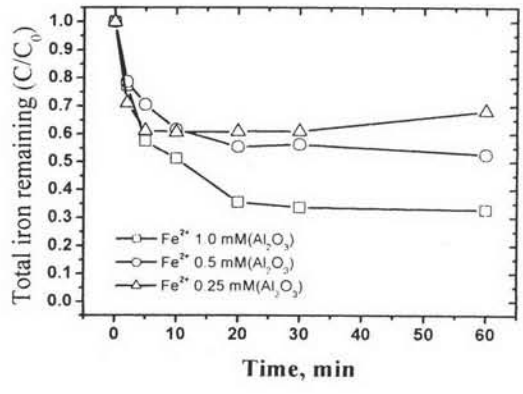

Figure 4.19d Total iron remaining.

Figure 4.19 Effect of ferrous ions on the oxidation of nitrobenzene in FBR of aluminium oxide media; 0.01 M of NB, 0.05 M of H_2O_2, 100 g/l of the Al_2O_3 and initial pH 2.8.

This process not only attains high nitrobenzene removal efficiency but also reduces the large amount of sludge being produce. Furthermore, FeOOH synthesized from the reaction of H_2O_2 and Fe^{2+} can also be used as the heterogeneous catalyst of H_2O_2. Even the nitrobenzene removal at higher ferrous concentration and lower ferrous concentration was no difference.

Form the Figure 4.19 illustrated that the total iron remaining in the condition with ferrous concentration 0.00025 M, 0.0005 M and 0.001 M of Al_2O_3 was 68.20%, 52.60% and, 32.80% respectively. Decreasing total iron remaining in the solution implied that crystallized iron coated onto the surface of carriers. From the results, the condition, high initial ferrous concentration (0.001 M of Fe^{2+}), the total iron remaining was 32.80% at 60 minutes. It indicated that ferric coated onto the surface of carriers via the crystallization about 67.20% of total iron concentration as shown in Figure 4.19d. As the cotinuous mode, the iron onto the surface of carriers can be used as heterogeneous catalyst and the amount of iron sludge was also reduced.

4.10 Effect of inorganic ions on the oxidation of nitrobenzene in fluidized-bed reactor.

4.10.1 Effect of dyhydrogen phosphate on the oxidation of nitrobenzene in FBR.

In this experiment, the effect of dyhydrogen phosphate for fluidized-bed Fenton process was examined for nitrobenzene oxidation in the fluidized-bed Fenton reactor. The dyhydrogen phosphate concentration was operated at free, 0.0015, 0.02 and 0.2M. In the Figure 4.20, the oxidation of nitrobenzene increased with decreasing of concentration of dyhydrogen phosphate. The removal efficiency of nitrobenzene in the presence of effect of dyhydrogen phosphate with concentration was operated at free, 0.0015, 0.02 and 0.2M were 93.70%, 50.07%, 46.50% and 44.90% respectively. The pseudo-second-order rate constants obtained under different experimental conditions are compared in Table 4.9; the reaction time for these experiments was

30 minutes. The good fit of the linear model to the data (R>0.92 in all cases) provides strong evidence that the reaction is pseudo-second order with respect to nitrobenzene concentration. The inhibition effect of dyhydrogen phosphate increased with increasing dyhydrogen phosphate concentration ranging from 0 to 0.2 M. The form which phosphate ions take on in a solution is determined by the cation species and the pH of the solution. From the pH-phosphate distribution diagram (Mattel, 1952), it can be seen that when pH=3, phosphate primarily exists in the form of $H_2PO_4^-$ which will react with ferrous and ferric ions to form complex compounds, as shown in equation 4-13 to 4-14;

$$Fe^{2+} + H_2PO_4^- \rightarrow FeH_2PO_4^+ \quad K = 10^{2.75} \qquad 4\text{-}13$$

$$Fe^{3+} + H_2PO_4^- \rightarrow FeH_2PO_4^{2+} \quad K = 10^{5.84} \qquad 4\text{-}14$$

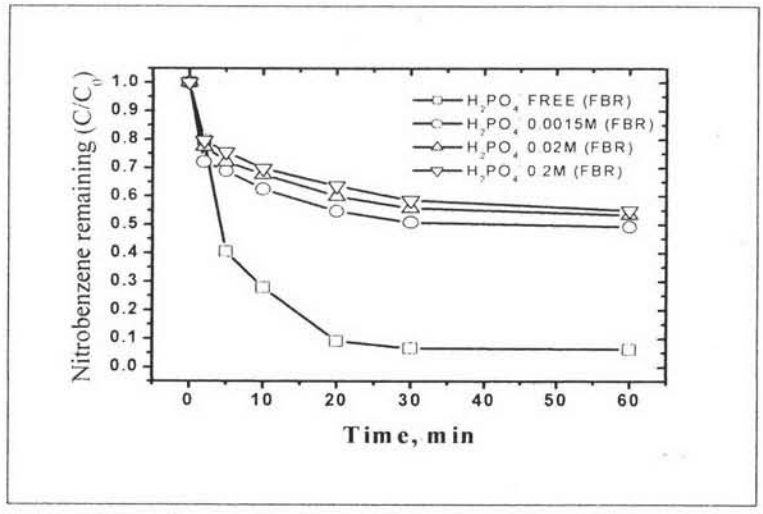

Figure 4.20 Effect of dyhydrogen phosphate: 0.01 M of NB, 0.001 M of Fe^{2+}, 0.05 M of H_2O_2, and initial pH 2.8.

It is still possible to oxidize nitrobenzene in the first stage. In the second stage, $FeH_2PO_4^{2+}$ reacts slowly, or does not react at all with hydrogen peroxide. Besides, the concentration of the free ferric ions remaining in the solution is too low, so that the decomposition reaction of nitrobenzene can not be observed.

Table 4.9 Pseudo-second order rate constants of nitrobenzene removal with effect of dyhydrogen phosphate.

$H_2PO_4^-$ (M)	Initial Rate (x 10^{-2} M.min^{-1})	Second-Order	
		k (x 10^{-2} $M^{-1}min^{-1}$)	R
0	10.10	49.21100	0.98888
0.0015	13.95	2.70600	0.92123
0.02	11.25	2.22100	0.92555
0.2	10.25	1.97000	0.92954

4.10.2 Effect of nitrate on the oxidation of nitrobenzene in FBR.

In this experiment, the effect of nitrate for fluidized-bed Fenton process was examined for nitrobenzene oxidation in the fluidized-bed Fenton reactor. The nitrate concentration was operated at free, 0.0015, 0.02 and 0.2M. In the Figure 4.21, the removal efficiency of nitrobenzene in the presence of effect of nitrate with concentration was operated at free, 0.0015, 0.02 and 0.2M were 93.70%, 93.50%, 93.60% and 92.40% respectively.

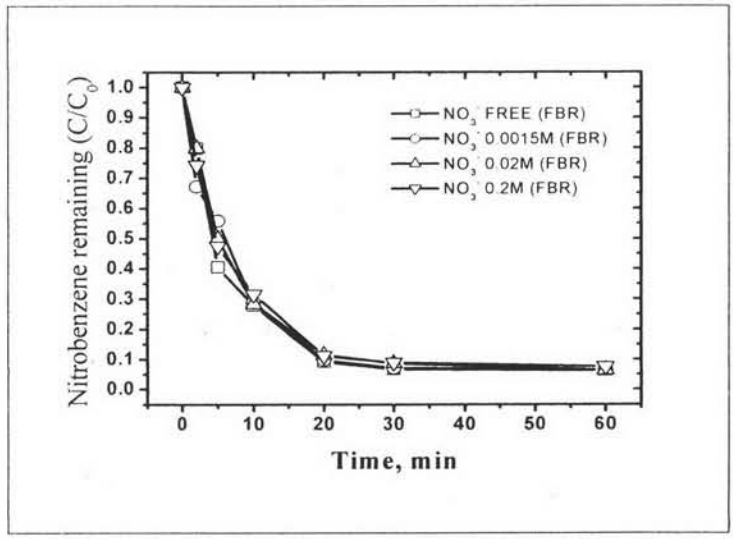

Figure 4.21 Effect of nitrate : 0.01 M of NB, 0.001 M of Fe^{2+}, 0.05 M of H_2O_2, and initial pH 2.8.

The pseudo-second order rate constants obtained under different experimental conditions are compared in Table 4.10; the reaction time for these

experiments was 30 minutes. The good fit of the linear model to the data (R>0.98 in all cases) provides strong evidence that the reaction is pseudo-second order with respect to nitrobenzene concentration. The inhibition effect of nitrate was not obvious, there are two reasons why; (1) NO_3^- will not produce a complex reaction with ferric ions, therefore. the reaction between ferric ions and hydrogen peroxide is not suppressed; (2) Because and NO_3^- will not react with hydroxyl radicals, the decompositon rate of nitrate was not inhibited.

Table 4.10 Pseudo-second-order rate constants of nitrobenzene removal with effect of nitrate.

NO_3^- (M)	Initial Rate (x 10^{-2} M.min^{-1})	Second-Order	
		k (x 10^{-2} $M^{-1}min^{-1}$)	R
0	10.10	49.21100	0.98888
0.0015	16.40	45.79800	0.98741
0.02	10.05	37.23700	0.99290
0.2	12.85	36.41900	0.98557

In conclusion, effect of inorganic ions on the oxidation of nitrobenzene in fluidized-bed reactor. Their order of sequence according to the reaction rate is: $H_2PO_4^-$ > > Cl^- > NO_3^-. When the background ion used is $H_2PO_4^-$, nitrobenzene was hardly decomposed at all during the second stage. The reason for this is that ferric ions undergo a complex reaction with $H_2PO_4^-$, causing ferric ions to lose the power to catalyze hydrogen peroxide. However, $FeH_2PO_4^+$ possibly reacts with hydrogen peroxide and produces radicals. It is still possible to oxidize nitrobenzene.

4.11 Effect of ferrous by COD analysis on the oxidation of nitrobenzene in FBR.

Although nitrobenzene was degraded more than 90% at the end of 60 minutes of the oxidation reaction with high ferrous ion concentration, it may be oxidized to other intermediates, which possibly have more toxic than parental compound. In this part was investigated the effect of ferrous by COD analysis on the oxidation of nitrobenzene in fluidized-bed Fenton process.

Therefore, experiments with increased initial ferrous ion concentration were carried out to investigate the removal of COD. The oxidation rate of nitrobenzene with different initial ferrous ion concentrations ranging from 2.5×10^{-4} M to 1.0×10^{-3} M. The removal efficiency of COD in fluidized-bed Fenton process in the presence of ferrous concentration at 0.00025M, 0.0005M and 0.001M were 23.74%, 28.28% and 34.50% respectively that were shown in Figure 4.22.

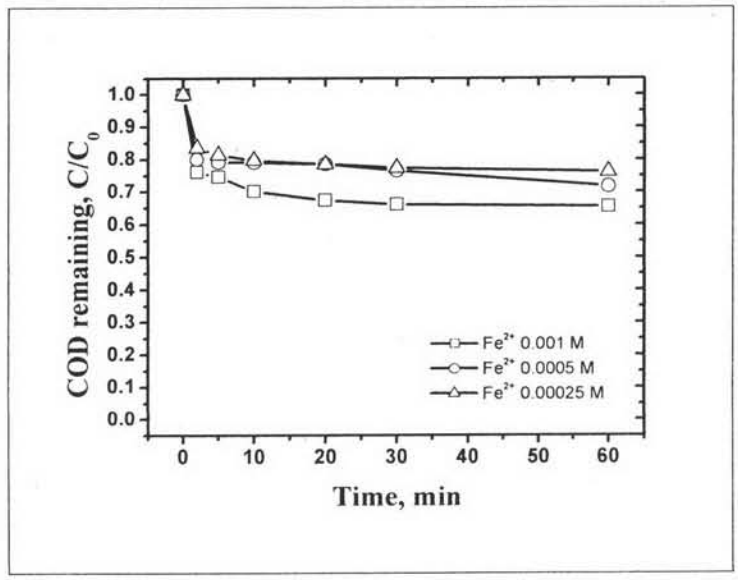

Figure 4.22 Effect of ferrous by COD analysis; 0.01 M of NB, 0.05 M of H_2O_2, 100 g/l of the aluminium oxide and initial pH 2.8.

In this experiments, the result show COD data with increased initial ferrous ion concentration were carried out to investigate. COD in the reaction mixtures decreased with increasing initial ferrous concentration but the removal efficiency still not enough in fluidized-bed Fenton process.